Supplementary Information

Grain Boundary Sliding and Amorphization is Responsible for Reverse Hall-Petch Relation in Superhard Nanocrystalline Boron Carbide

Dezhou Guo[1+], Shuangxi Song[2+], Ruichun Luo[2], William A. Goddard III,[3] Mingwei Chen[2,4], Kolan Madhav Reddy[2*], and Qi An[1,5*]

[1]Department of Chemical and Materials Engineering, University of Nevada Reno, Reno, Nevada 89557, USA

[2]State Key Laboratory of Metal Matrix Composites, School of Materials Science and Engineering, Shanghai Jiao Tong University, Shanghai 200240, China.

[3]Materials and Process Simulation Center, California Institute of Technology, Pasadena, California 91125, United States

[4]Department of Materials Science and Engineering, Johns Hopkins University, Baltimore, MD 21218, USA.

[5]Nevada Institute for Sustainability, University of Nevada, Reno, Reno, Nevada, 89557, USA

+ These authors are equal contributions

*Corresponding Author E-mail: qia@unr.edu, kmreddy@sjtu.edu.cn

METHODS

Computational details.

Our simulations use the QM-based ReaxFF reactive force field incorporated into the large-scale atomic/molecular massively parallel simulator (LAMMPS)[1] software. ReaxFF has accurately predicted the amorphous shear band formation in B_4C along predicted slip systems[2]. Here we find shear deformation induced grain boundary failure mechanism and grain size effects.

The GB models are constructed using the Voronoi construction approach. First, the seeds are inserted in the super cell and each seed is associated with a rotation matrix to rotate the grain about the seed. Then each grain around the seed is cut out by the Voronoi polygon. Finally these grains are pasted together to form the polycrystalline materials as shown in Fig. S1. Fig. S1 displays three n-GBs models: (1) GB1 with grain size of 4.48 nm and 135,050 atoms; (2) GB2 with grain size of 9.74 nm containing 1,092,685 atoms; and (3) GB2 with grain size of 14.64 nm and 3,702,861 atoms. The atomic positions and cell parameters are first optimized to minimize the potential energy and geometries. To equilibrate the GB atoms, the GBs models are annealed from 1000 K to room temperature within 500 ps using NPT ensemble (constant pressure, constant temperature and constant number of atoms). Then we carried out isothermal–isobaric (NPT) RMD simulations until the system relaxed the internal stresses to zero at ambient conditions. Here, we used the Nose–Hoover thermostat and barostat (100 fs damping constant for temperature and 1000 fs dumping constant for pressure). The periodic boundary conditions are applied along all three directions and the integration time step was set to 0.25 fs. The equilibrium density from ReaxFF is ρ_0 = 2.58 g·cm^{-3}, in reasonable agreement with the experimental value of 2.52 g·cm^{-3} at 300 K.

After obtaining the equilibrium structure at ambient conditions, we applied shear

deformations on all three GB models to examine the mechanical response of n-B_4C. We sheared the system along the x−z plane until failure at a constant shear rate of 0.1 ps^{-1}. The NVT ensemble was applied during the shear deformation. Here, we used the Nose–Hoover thermostat (100 fs damping constant) in NVT MD simulations.

To analysis the GB sliding at the atomic level, we apply the atomic local shear strain mises. For each atom, calculation of atomic strain requires two atomic configurations, one current and one reference, which is a good measure of local inelastic deformation.

Experiment Details

Material fabrication and mechanical testing. Bulk Nanocrystalline B_4C ceramic was consolidated at a temperature of 1600 ^oC and a pressure of 1.0 GPa for a time of 1h using Hot Isostatic Pressing (HIP)[3]. The relative density of the synthesized bulk n-B_4C is around ~93% of the theoretical value, suggesting that the remaining volume is accompanied by free carbon and fine nanoporosity. A mirror finish surface was prepared by careful polishing with diamond films prior to mechanical testing. A series of nanoindentation tests were carried out at a constant depth of 1000 nm using depth controlled Nano indenter G200 (MTS Systems Ltd) equipped with Berkovich indenter. The creep measurement was performed using a Hysitron Ti-950 nanoindenter equipped with a Berkovich tip.

Microstructural characterization. The freestanding cantilever beam with width b = 12 μm, length L = 49 μm, and thickness t = 6.5μm was machined from a bulk n-B_4C sample using a focused ion beam (FIB) system (FEI Versa3D) integrated with high resolution SEM imaging. The cross sectional TEM specimens of indented n-B_4C were prepared using the same FIB system. Prior to TEM observations, the FIB cross sectioned n-B_4C samples were gently milled by the Fishone 1040 Nanomill system at 500 eV to remove Ga^+ contamination without altering the

specimen chemistry and structure. The microstructure of deformed region samples was characterized using JEOL-ARM 200F atomic resolution analytical microscope equipped with a Cs corrector, operated at an acceleration voltage of 200 kV. The ABF-STEM images were recorded using JEOL BF detector with the detector angle range of 11-23 mrad.

Von-Mises shear strain calculation

To quantify the local plastic deformation during the shear process, we computed the Von-Mises shear strain n_i^{Mises} for each atom. This measure was incorporated into visualization program AtomEye. The calculation of n_i^{Mises} requires two atomic configurations, one current, and one reference. A local transformation matrix J_i are sought which best maps

$$\{\boldsymbol{d}_{ji}^0\} \rightarrow \{\boldsymbol{d}_{ji}\}, \forall j \in N_i^0 \tag{1}$$

where d's are vector separations between atom j and i (superscript 0 means the reference configuration). j is one of atom i's nearest neighbors, and N_i^0 is the total number of nearest neighbors of atom i, at the reference configuration. J_i is determined by minimizing

$$\sum_{j\in N_i^0} |\boldsymbol{d}_{ji}^0 \boldsymbol{J}_i - \boldsymbol{d}_{ji}|^2 \rightarrow \boldsymbol{J}_i \left(\sum_{j\in N_i^0} \boldsymbol{d}_{ji}^{0T} \boldsymbol{d}_{ji}^0\right)^{-1} \left(\sum_{j\in N_i^0} \boldsymbol{d}_{ji}^{0T} \boldsymbol{d}_{ji}^0\right) \tag{2}$$

For each J_i, the local Lagrangian strain matrix is computed as

$$n_i = \frac{1}{2}(J_i J_i^T - I) \tag{3}$$

Then atom i's local shear invariant can be computed as

$$\boldsymbol{n}_i^{Mises} = \sqrt{n_{yz}^2 + n_{yz}^2 + n_{yz}^2 + \frac{(n_{yy}-n_{zz})^2 + (n_{xx}-n_{zz})^2 + (n_{xx}-n_{yy})^2}{6}} \tag{4}$$

Local stress calculation

We obtained the local shear stress by summing up the atomic stresses of all atoms in the triple-junction region, as shown in Fig.2. The atomic stresses are computed using the virial stress including the kinetic contribution and potential contribution [4, 5].

During the shear process, the local shear stress distributions are heterogeneous instead of homogeneous because of the different deformation response between atoms in crystalline parts

and in grain boundary regions. In the shear process, the atoms in GB regions have experienced deconstruction of icosahedral clusters, amorphization and cavitation, while in crystalline region, the atoms only undergo an elastic deformation. As a result, although the local stress of this grain boundary region relaxes to 0 with significantly density decreasing for the cavitation at 0.5 strain, the total stress of the whole system is about ~20 GPa.

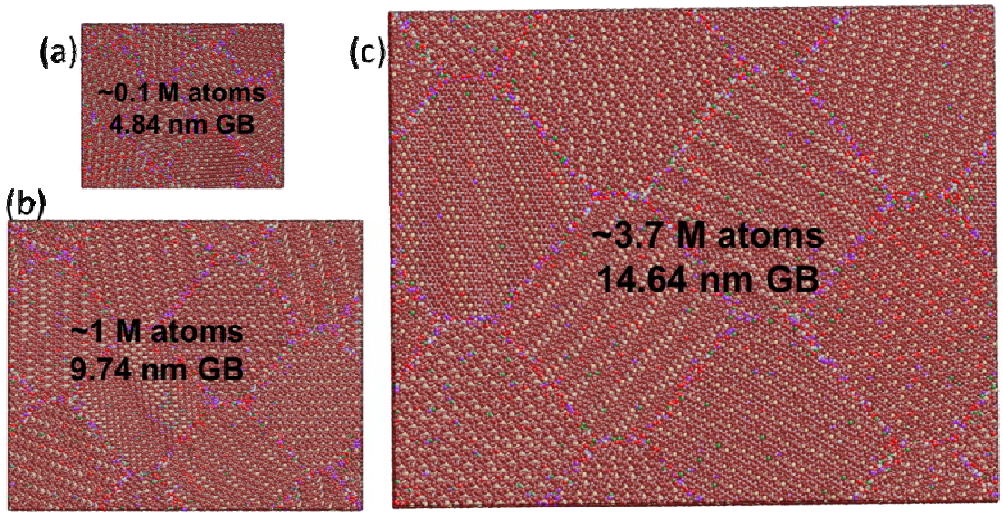

Figure. S1 Three simulation models of nanocrystalline B_4C with 16 randomly oriented grains arranged on a BCC lattice. (a) Grain boundary model 1 (GB1) including 135050 atoms with 4.48 nm grain size; (b) Grain boundary model 2 (GB2) containing 1092685 atoms with 9.74 nm grain size; (c) Grain boundary model 3 (GB3) containing 3702861 atoms with 14.64 nm grain size.

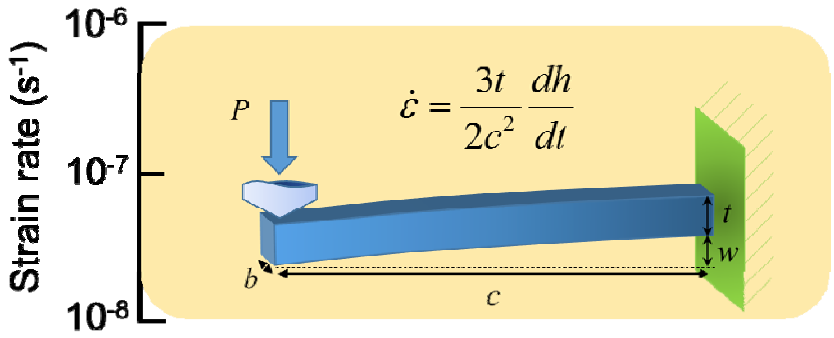

Figure. S2 Schematic drawing of cantilever bending creep measurement using nanoindenter.

Cantilever with width b = 12μm, length L = 49μm, and thickness t = 6.5μm is machined from a bulk nanocrystalline Boron carbide sample using FIB. The creep measurement is performed using a Hysitron Ti-950 nanoindenter equipped with a Berkovich tip. The experimental set up is shown in Fig. 3 schematically. The distance between the indenter tip and the pivot point of the cantilever is c = 45μm. During the test, the indenter probe first contacted the cantilever with 1 μN force for 200 seconds thermal drift monitoring, and then loaded with constant force P = 5 mN as long as 1000 seconds for creep measurement, following by a 1000 seconds recovering and thermal drift monitoring with 1 μN contact force. The deflection displacement at the indenter tip as a function of time during the creep test is plotted in Fig. 3 after thermal drift compensation. It is clear there is creep deformation at the pivot point of the cantilever during the loading segment, while the recovery is instantly elastic. The enlarged view of the creep segment is shown in Fig. 3, in which the creep rates reach to a constant rate about 0.01 nm/s.

The load that the cantilever fractured is 6.145 mN and defined as the fracture load, P_f, and the fracture strength is given by following equation.

$$\sigma_f = 6cP_f \Big/ \left(bt^2\right)$$ Equation (1)

The fracture strength is calculated to be 3.3 GPa which is much lower than the theoretic yielding strength of this material which is about 1/3 of indentation hardness σ_y = H/3 = 6.6 GPa. The under estimated fracture strength is mainly because of pores within the material indicated by red arrows in Fig. 3 (c-e).

The instantaneous elastic strain at 5 mN load is determined by Eq. (2) and the creep strain rate can be estimated by Eq. (3).

$$\varepsilon_0 = \frac{6Pc}{bt^2E} = 0.0168$$ Equation (2)

$$\dot{\varepsilon} = \frac{3t}{2c^2}\frac{dw}{dt}$$ Equation (3)

Therefore, the creep strain is plotted as a function of time in Fig. 3 (e) and Fig S3.

The steady-state displacement rate during constant 5 mN load is about 0.01 nm/s as shown in Fig. 3 and Fig. S3. The creep stress is about 2.6 GPa from Eq. (1). Therefore, the creep strain rate at 2.6GPa or $0.81\sigma_f$ or $0.4\ \sigma_y$ is estimated as $4.8\times 10^{-8}\ s^{-1}$.

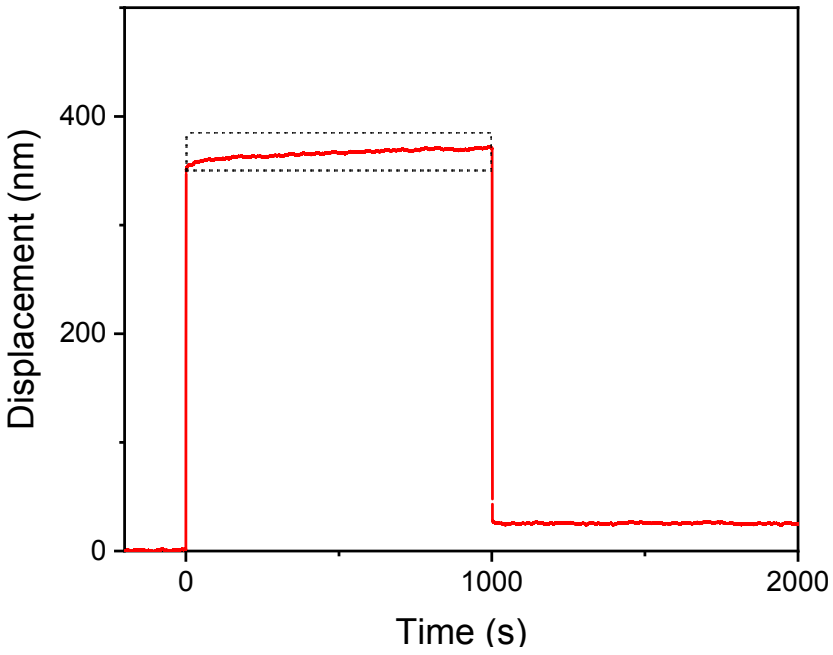

Figure S3. Displacement of indenter as a function of time in a 5 mN constant load cantilever bending measurement.

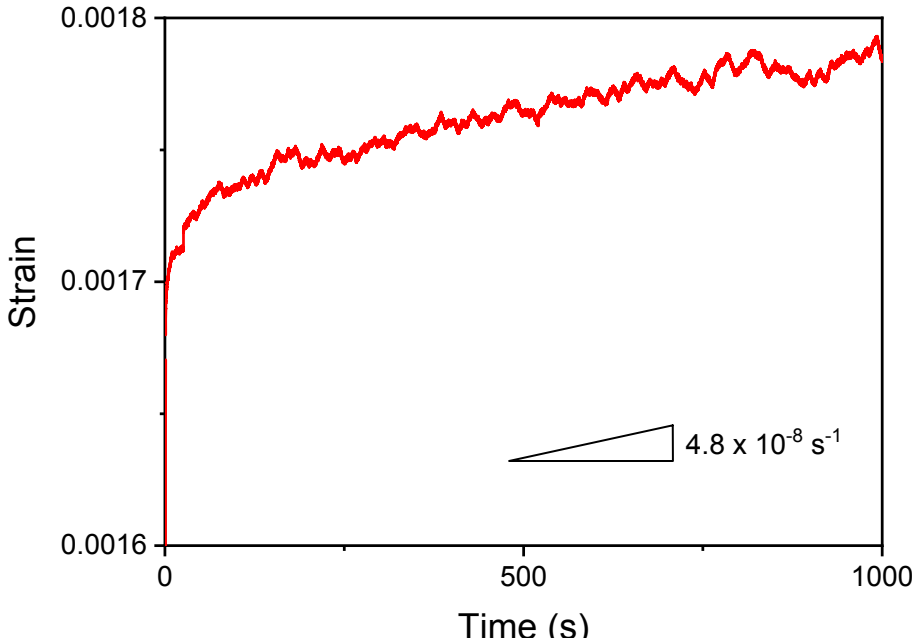

Figure S4. Calculated creep strain as a function of time for the cantilever under 5 mN constant force. Triangle with slope of 4.8×10^{-8} s^{-1} is shown for reference.

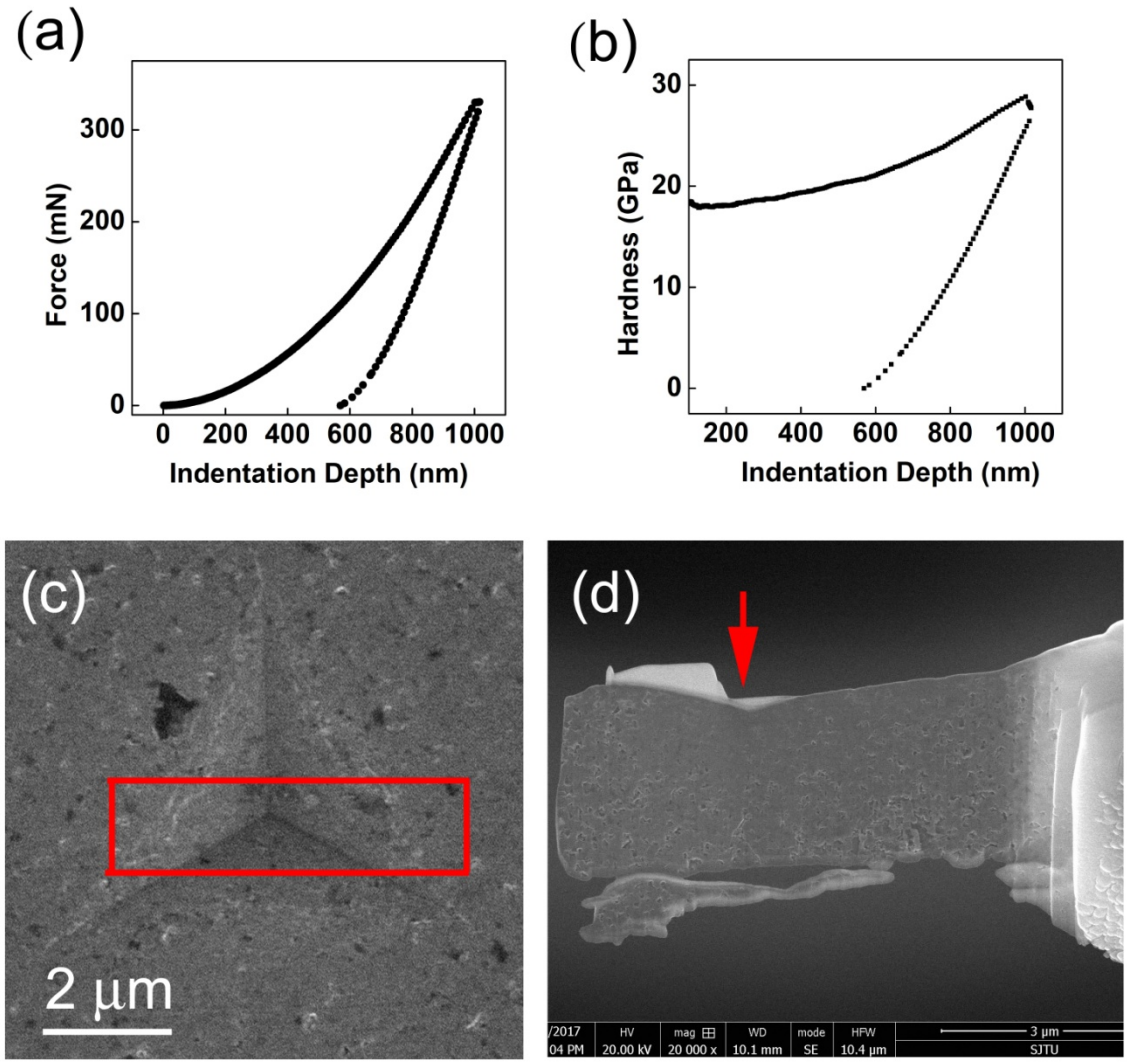

Fig. S5 Depth controlled nanoindentation testing and microstructural characterization of TEM sample preparation. (a) Typical load-depth curve applied with maximum depth of 1000 nm. (b) Hardness vs indentation depth of n-B_4C (c) SEM image of Indented n-B_4C region (d) SEM image of FIB sliced sample for TEM observations. Arrow head shows indentation projection.

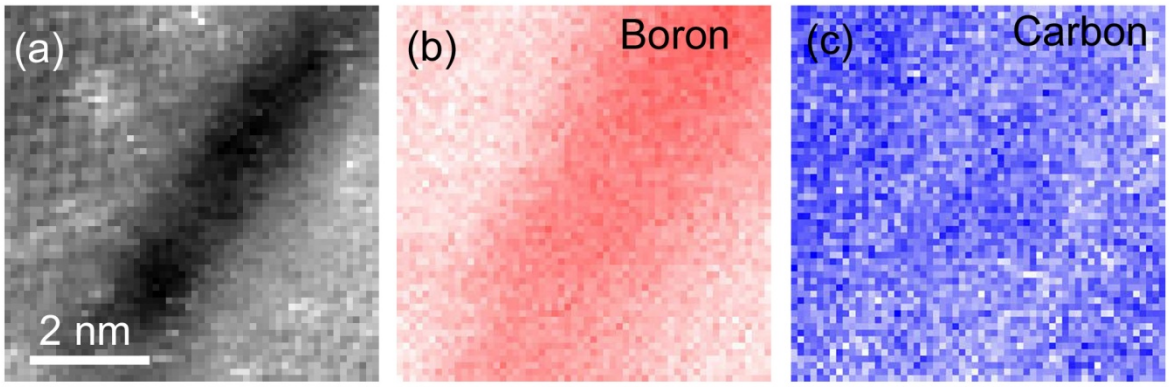

Fig. S6 STEM EELS of chemical mappings of amorphous interface in deformed n-B_4C. (a) Dark field STEM image acquired of interface in between n-B4C grains. (b) Boron (B) mapping and (c) Carbon (C) mapping shows chemical homogeneity of B and C in both interface and n-B_4C grains.

REFERENCES

[1] S. Plimpton, J. Comput. Phys. **117**, 1-19 (1995).

[2] I. Szlufarska, A. Nakano, P. Vashishta, Science **309**, 911-914 (2005).

[3] K. Madhav Reddy, J.J. Guo, Y. Shinoda, T. Fujita, A. Hirata, J.P. Singh, J.W. McCauley, M.W. Chen, Nat. Commun. **3**, 1052 (2012).

[4] M. Zhou, Proc. Roy. Soc. Lond. A. **459**, 2347-2392 (2003).

[5] A.K. Subramaniyan, C.T. Sun, Int. J. Solids Struct. **45**, 4340-4346 (2008).